

DETECTION OF CORN KERNELS INFECTED BY FUNGI

T. C. Pearson, D. T. Wicklow

ABSTRACT. Single-kernel reflectance spectra (550 to 1700 nm), visible color reflectance images, x-ray images, multi-spectral transmittance images (visible and NIR), and physical properties (mass, length, width, thickness, and cross-sectional area) were analyzed to determine if they could be used to detect fungal-infected corn kernels. Kernels were collected from corn ears inoculated with one of several different common fungi several weeks before harvest, and then collected at harvest time. It was found that two NIR reflectance spectral bands centered at 715 nm and 965 nm could correctly identify 98.1% of asymptomatic kernels and 96.6% of kernels showing extensive discoloration and infected with *Aspergillus flavus*, *Aspergillus niger*, *Diplodia maydis*, *Fusarium graminearum*, *Fusarium verticillioides*, or *Trichoderma viride*. These two spectral bands can easily be implemented on high-speed sorting machines for removal of fungal-damaged grain. Histogram features from three transmittance images (blue and red components of color images and another at 960 nm) can distinguish 91.9% of infected kernels with extensive discoloration from 96.2% of asymptomatic kernels. Similar classification accuracies were achieved using x-ray images and physical properties (kernel thickness, weight, length). A neural network was trained to identify infecting fungal species on single kernels using principle components of the reflectance spectra as input features.

Keywords. Aflatoxin, Corn, Detection, Feature selection, Fumonisin, Image, Maize pathogens, Near-infrared.

Fungal-infected maize (*Zea mays* L.) kernels are classified by plant pathologists according to type of disease symptoms produced, including kernel or ear rots, streaked or blotched kernels, etc., and their ecology (Wicklow et al., 1980; Samuels, 1984; Smith et al., 1988; Wicklow, 1995; White, 1999). Kernel symptom expression is a product of infecting fungal species, drought stress, and nutritional deficiencies (White, 1999). Reactions associated with maize varietal resistance or susceptibility can also contribute to the symptomology of infected grain (Wright and Billeter, 1974; Hart et al., 1984; Lambert and White, 1997; Walker and White, 2001; Naidoo et al., 2002; Clements et al., 2003). Seed color and form changes, detectable visually, are actually preceded by chemical changes in the grains caused by the fungus. For example, *Aspergillus flavus* initially infects the oil-rich germ using grain lipids for its growth and metabolism, and thus lipid hydrolysis takes place faster than the degradation of protein or starch in stored grain (Sauer and Christensen, 1969; Wacowicz, 1991; Pomeranz, 1992). Lipids are broken down by lipases to free fatty acids and glycerol; thus, the free fatty acid content of grain has been proposed as a sensitive index of incipient grain deterioration (Christensen and Kaufmann, 1969; Faraq et al., 1981; Richard-Molard, 1988; Pomeranz, 1992). Other more common species of kernel-rotting fungi (e.g., *Fusarium verticil-*

lioides, *Fusarium graminearum*, *Stenocarpella maydis* (syn. *Diplodia maydis*), *Trichoderma viride*, *Nigrospora oryzae*, *Penicillium oxalicum*, etc.) may enter the seed proper based on a different pathology and in earlier stages of kernel development, producing different symptoms of kernel infection (Clayton, 1927; Johann, 1935; Koehler, 1942; Caldwell et al., 1981; Lawrence et al., 1981; Sutton, 1982; Bennett et al., 1988; Smart et al., 1990; Klapproth and Hawk, 1991; Munkvold et al., 1997). These fungi can reduce yield, quality, and nutritional value of the grain, while also contaminating it with fungal-derived chemicals, some of which are recognized as mycotoxins because of their deleterious biological effects in animals and humans (Richard and Payne, 2003). Mycotoxin contamination of grain can result in substantial economic losses to maize growers, livestock and poultry producers, grain handlers, and food and feed processors.

While corn kernels infected with fungi are more friable and may have reduced densities (Shotwell et al., 1974; Shetty and Bhat, 1999), it has been shown that grain cleaning will not greatly reduce aflatoxin or fumonisin levels in commercially harvested corn (Brekke et al., 1975; Pearson et al., 2004). Near-infrared transmittance (NIRT) and near-infrared reflectance (NIRR) spectroscopy have been used to evaluate internal quality of many whole grains and nuts. It has been shown that only a few absorbance bands in the visible and near-infrared spectrum can detect whole corn kernels highly contaminated in the field with aflatoxin (Pearson et al., 2001) and fumonisin (Dowell et al., 2002). Continuing with this work, Pearson et al. (2004) used NIR spectra to optimize a dual-band, high-speed optical sorter for removing whole corn kernels contaminated with aflatoxin and fumonisin. This method was able to reduce aflatoxin by an average of 81% and fumonisin by 85% for corn grown in Kansas. However, no effort has been made to investigate the feasibility of this technique for removing infected kernels in general or distinguishing kernels infected by different species. Given that fungal-damaged kernels are of low quality and may have

Submitted for review in November 2005 as manuscript number IET 6182; approved for publication by the Information & Electrical Technologies Division of ASABE in June 2006.

The authors are **Thomas C. Pearson**, ASABE Member Engineer, Agricultural Engineer, USDA-ARS Grain Marketing Research and Production Research Center, Manhattan, Kansas; and **Donald T. Wicklow**, Research Microbiologist, USDA-ARS National Center for Agricultural Utilization Research, Peoria, Illinois. **Corresponding author:** Thomas C. Pearson, USDA-ARS Grain Marketing Research and Production Research Center, 1515 College Ave., Manhattan, KS 66502; phone: 785-776-2729; fax: 785-537-5550; e-mail: tpearson@gmprc.ksu.edu.

undesirable traits besides containing mycotoxins, overall corn quality may be improved further by removing all fungal-damaged kernels through optical sorting. Furthermore, breeders attempting to investigate resistance to fungi need rapid methods for identifying fungal-infected kernels and, ideally, the species infecting each kernel.

OBJECTIVE

The purpose of this study was twofold:

- Determine if corn kernels infected with one of several common fungi could be distinguished from un-infected kernels by physical properties, imaging methods, or with a pair of spectral bands as used in high-speed (~1000 kernels/s) optical sorters. In regards to high-speed optical sorting, the purpose was to identify spectral bands that are optimal for identifying corn kernels infected with a plurality of fungi rather than just a specific fungi, as was done by Pearson et al. (2004).
- It was also desired to identify species of the infecting fungi using full NIR spectra so that infected kernels could be separated at low speed (~1 kernel/s) using automated, full-spectrum, commercial NIR machines such as those currently marketed by Brimrose Corporation (Baltimore, Md.) and Perten Instruments (Springfield, Ill.).

MATERIALS AND METHODS

Reflectance spectra (550-1700 nm), visible color reflectance images, x-ray images, multi-spectral transmittance images, and physical properties (mass, thickness, and cross-sectional area) of fungi-infected and non-infected corn kernels were analyzed for their ability to identify fungal-infected kernels. Samples originated from field-inoculated corn. After harvest, measurements of all kernels were taken, followed by incubation, and infecting species identification. Each step in this process is explained in the following sections.

FUNGAL INOCULATIONS OF CORN HYBRIDS

Corn kernels used in this study were collected from ears that were wound-inoculated per Wicklow (1995) with one of

the fungi listed in table 1. Inoculations were performed in the late milk to early dough stage of kernel maturity for two commercial corn hybrids grown at Kilbourne, Illinois, in 2001 (Pioneer hybrid P-3394) and in 2002 (Farm Service hybrid FS-7111). Another source for *A. flavus* infected samples consisted of grain from ears of Pioneer 3394 that were inoculated with *A. flavus* in 1997 (Pearson et al., 2004). Shortly after harvest, the corn kernels were examined and separated into one of the following categories based on their visual characteristics: (1) “extensive discoloration” of 50% or more of the kernel surface, (2) “minor discoloration” of less than 50% of the kernel surface, and (3) no visible kernel damage (asymptomatic). The actual wound-inoculated kernels were discarded so that only those kernels where the fungus spread naturally were studied. Friable kernels and fragments were not included in this study as they are usually removed by existing cleaning equipment at grain elevators. A total of 1222 P-3394 kernels and 1120 FS-7111 kernels were used for this study. Table 1 lists the number of kernels used from each fungus and damage category. A total of 292 and 148 asymptomatic kernels were selected from the Pioneer and Farm Service hybrids, respectively.

SINGLE-KERNEL MEASUREMENTS

NIR Reflectance Measurement

Whole-kernel reflectance spectra from 500 to 1700 nm were measured using a diode-array near-infrared spectrometer (DA7000, Perten Instruments, Springfield, Ill.). The spectrometer measures absorbance using an array of silicon (7 nm resolution) and indium-gallium-arsenide sensors (11 nm resolution). The spectrometer sampled 15 spectra and stored the average. Each spectrum was collected in 33 ms; thus, 0.495 s was required for capturing all 15 spectra.

Kernels were manually placed on a bifurcated inter-actance probe attached to the spectrometer and light source (fig. 1). The viewing area was 17 mm in diameter and 10 mm above the termination of the illumination and reflectance fibers. The illumination bundle was a 7 mm diameter ring, and the reflectance probe bundle was 2 mm in diameter. Spectra were obtained of all kernels oriented at the germdown position (germ facing the optical fiber bundle), and then a second set of spectra was collected for all kernels that

Table 1. Numbers of maize kernels selected showing minor versus extensive symptoms of kernel discoloration resulting from infection by common species of kernel-rotting fungi.^[a]

Infecting Fungus	Symptoms of Kernel Discoloration			
	Pioneer 3394 ^[b]		FS 7111 ^[c]	
	Minor	Extensive	Minor	Extensive
<i>Acremonium zeae</i> NRRL 6415, NRRL 13540, NRRL 13541	53	14	36	5
<i>Aspergillus flavus</i> NRRL 32355	299	148	38	59
<i>Aspergillus niger</i> NRRL 6411	40	12	0	52
<i>Diplodia maydis</i> NRRL 13615, NRRL 31249	112	71	69	100
<i>Fusarium graminearum</i> NRRL 13188, NRRL 31250	35	34	38	31
<i>Fusarium verticillioides</i> NRRL 25457	131	36	274	176
<i>Nigrospora oryzae</i> NRRL 6414	--	--	--	--
<i>Penicillium</i> spp.	26	34	19	57
<i>P. pinophilum</i> (syn. <i>P. funiculosum</i>) NRRL 6420	--	--	--	--
<i>P. oxalicum</i> NRRL 6416	--	--	--	--
<i>Trichoderma viride</i> NRRL 6418	107	70	86	80
Total	803	419	560	560

^[a] Kernels were selected from ears that were wound-inoculated with individual fungi, and the infecting species was confirmed by kernel platings.

^[b] Pioneer 3394 maize hybrid grown at the University of Illinois River Valley Sand Farm, Kilbourne, Illinois, 1997 and 2001.

^[c] FS 7111 maize hybrid grown in a commercial farm field, Kilbourne, Illinois, 2002.

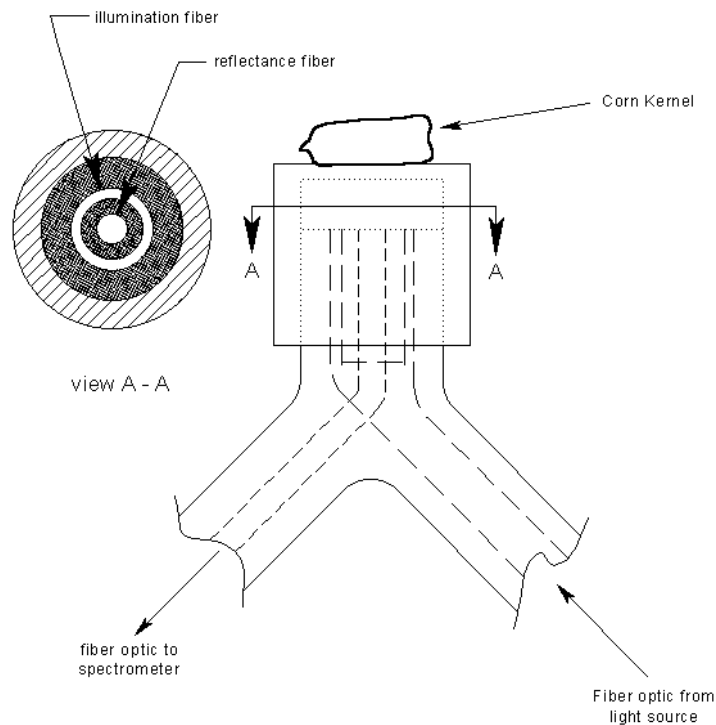


Figure 1. Reflectance sampling apparatus.

were viewed germ-up. The spectra were stored on a hard disk for subsequent analysis.

Imaging

Visible color reflectance images, x-ray images, and multi-spectral transmittance images were taken of all kernels. For all image types except x-ray images, two sets of images were acquired, one with the kernels oriented with their germ facing the image sensor and the other with the germ away from the image sensor. Kernels were placed onto adhesive-backed plastic sheets in sets of 30 per sheet and imaged together. Care was taken so that the kernels were not touching each other. Every image utilized a white and black standard to ensure that the intensities of all images were of a consistent scale. Details of image pixel intensity standardization are discussed in detail below.

Visible and NIR Transmittance Image Measurement

Multi-spectral transmittance images were acquired by coupling a small camera (QuickCam Pro 3000, Logitech, Fremont, Cal.) to a filter wheel to allow rapid acquisition of 12 different images at different spectral bands. The near-infrared blocking filter mounted onto the camera was removed to allow images in the near-infrared spectrum to be acquired. Eleven of the 12 filters used on the filter wheel were interference filters allowing a 10 nm full-width, half-maximum (FWHM) band of light to pass through. The remaining filter was a near-infrared blocking filter to allow acquisition of color images. Pass bands of the interference filters were centered at 780, 830, 870, 880, 890, 905, 920, 930, 960, 980, and 1020 nm. Resolution of the camera was 640×480 pixels. A 12 mm focal length lens (F54-854, Edmund Industrial Optics, Barrington, N.J.) was fitted onto the camera so that the entire area of an 80×95 mm backlight (QVABL, Dolan Jenner Industries, Inc., Lawrence, Mass.) could be kept in focus. The backlight was illuminated with a 250 W fiber optic

light source (1250, Cuda Products, Jacksonville, Fla.). A typical kernel contained nearly 2200 pixels and was approximately 40 pixels wide and 60 pixels tall.

The red, green, and blue components of the color transmittance image were split to form three gray-scale images representing their respective color components. For the NIR images, the three color channels were averaged to form one gray-scale image for that particular NIR band. A total of 14 gray-scale images representing different bands of light from the blue region of the visible spectrum to 1020 nm were acquired.

Two neutral-density filters with optical densities of 1.5 and 3.0 (F47-209 and F47-212, Edmund Industrial Optics, Barrington, N.J.) were permanently placed on the backlight and imaged with every set of kernels to provide a means to ensure that all images were of a consistent gray level. Average pixel intensities corresponding to the two neutral-density filters were used to histogram-stretch kernel images between 0 and 255. All kernel pixels had intensities between 20 and 220 after this operation.

Color Reflectance Imaging

A sheet containing 30 kernels was placed on a scanner (Expression 1680, Epson America, Long Beach, Cal.) and scanned at a spatial resolution of 300 pixels per inch and 8 bits per red, green, and blue channel. A gray-scale target (F53-712, Edmund Industrial Optics, Barrington, N.J.) was imaged with each set of kernels to ensure consistent light-intensity levels in the images. Each red, green, and blue channel of the images was split from the color image and histogram-stretched so that the average of the white standard represented 255, while the average of the black standard represented 0.

X-Ray Imaging

Kernels were radiographed using a cabinet x-ray system (43855A, Faxitron Corp, Wheeling, Ill.) with 13×18 cm

film (Kodak Industry M film, France) at an exposure of 18 kV and 3 mA for 2 min. The x-ray film was digitally scanned at 800 pixels/inch (Expression 1680, Epson America, Long Beach, Cal.) and the images were saved for analysis. Pieces of clear Lexan of 1.7, 3.4, 5.1, 6.8, and 8.5 mm thicknesses were placed on top of each x-ray film to ensure that the exposure was consistent. All corn kernels had pixel intensities between the average of the 1.7 mm and 8.5 mm thick Lexan pieces. Therefore, all images were histogram-stretched so that the average of the 8.5 mm piece was zero and the average of the 1.7 mm piece was 255.

Physical Property Measurement

Kernel thickness was measured with digital calipers (54-115-333, Fowler Tools and Instruments, Boston, Mass.) mounted on a horizontal platform. A single kernel was placed on the platform, germ side up, and then measured at the thickest point. Each kernel weight was measured on a digital balance (40SM-200A, Precisa, Switzerland), one kernel at a time.

FUNGAL EVALUATIONS

After all measurements were taken, the infecting species was identified. Kernels were surface disinfected with 2% Clorox and then plated on 3% malt extract agar. The fungus, if any, grown out from individual plated kernels was identified under a microscope and recorded. This fungus was used as the infecting species for NIR calibrations to identify infecting species on whole corn kernels.

DATA ANALYSIS

Selection of Spectral Bands for Sorting

The spectra were interpolated using Perten Simplicity software to 5 nm resolution from 500 to 1700 nm, resulting in 241 absorbance values. When considering the possible application of the results to high-speed sorting operations, only a few of the spectral bands can be economically measured in real time. Many modern sorting machines (e.g., Satake USA, Houston, Texas; Sortex, Ltd., London, U.K., etc.) are capable of measuring two discrete spectral bands (using optical filters) on two or three sides of a kernel, and then determining acceptance or rejection of a kernel based on one or more readings. As such, it was attempted to select the best single band and combination of two spectral bands to classify kernels as fungal positive or negative using spectra from both germ-up and germ-down kernel orientations.

The spectra were convolved with Gaussian curves to simulate different FWHM pass-band interference filters. A k-nearest neighbor classification scheme was used as the basis of a procedure to select an optimal small subset of spectral bands for sorting a given "good" product and "defect." An exhaustive search was performed for the best pair of spectral bands between 500 and 1700 nm. The selection procedure had an additional constraint that the spectral bands needed to be separated by at least 100 nm, as this is the usual limitation of the optics in sorting machines.

In searching for the best pair of spectral bands in the 241 spectral bands from the normalized spectra, a randomly selected sample of 30 good kernels and 30 extensively discolored kernels was used as a training set, with the remaining 886 kernels (356 kernels of P-3394 plus 530 kernels of FS-7111) used as a validation set. Every kernel had

two spectra associated with it, one from the endosperm side and the other from the germ side. Thus, the training set comprised 120 spectra from 60 samples. For each absorbance value in the Gaussian-smoothed spectra, the mean and standard deviation were computed for all kernels in the training set. All absorbance values were then normalized by subtracting the mean and dividing by the standard deviation:

$$A_{N\lambda} = \frac{(A_{\lambda} - \bar{A}_{\lambda})}{\sigma_{\lambda}} \quad (1)$$

where $A_{N\lambda}$ is the normalized absorbance centered at wavelength λ , A_{λ} is the Gaussian-smoothed absorbance centered at wavelength λ , \bar{A}_{λ} is the training set mean of the Gaussian-smoothed absorbance centered at wavelength λ , and σ_{λ} is the training set standard deviation at wavelength λ .

For each spectrum in the validation set, the Euclidian distance from a given pair of spectral bands was computed to the corresponding pair of spectral bands in the training set. This combination was performed for every possible pair of spectral bands with the limitation that they were at least 100 nm apart. After performing these computations for every pair of spectral bands, each kernel in the validation set had two distances to every kernel in the training set; one was the distance from the germ side and the other was from the endosperm side of the kernel. Classification was performed based on two different sorting cases. One case, called AND logic, required that the distance from both germ and endosperm spectra from each kernel be closest to a fungal-damaged kernel in the training set to be classified as fungal damaged; otherwise, it was classified as asymptomatic. The other case, called OR logic, only required that the distance from either the germ or endosperm spectra be closest to a fungal-damaged kernel in order for a kernel to be classified as fungal damaged. Most optical sorting machines can be set to sort based on AND as well as OR logic. The pair of spectral bands achieving the lowest classification error rate using this procedure was chosen as the optimal pair of bands that might be used in a sorting operation.

While AND logic tends to prevent asymptomatic kernels from being misclassified as damaged, OR logic is more likely to correctly classify kernels that have damage on only one side. For training purposes, it was only attempted to distinguish kernels with extensive discoloration from asymptomatic kernels. Classification of kernels with minor discoloration into either the asymptomatic or extensively discolored group was tested only after the classification model was developed.

Classification Using Stepwise Discriminant Analysis

In all images, kernels were segregated from the background by thresholding. One threshold level was used for each image modality. Features extracted from each kernel in every image were mean kernel pixel intensity, pixel intensity standard deviation, maximum pixel intensity, minimum pixel intensity, and a cumulative histogram of pixel intensities in steps of 16 intensity levels. The histograms were scaled to represent percentages of pixel intensities below each histogram bin level. Data from the germ and endosperm sides of each kernel were averaged and saved for analysis. The cross-sectional area, kernel length, and kernel width were also extracted from the blue component of the transmittance images.

All image data (x-ray, NIR transmittance, color reflectance), physical property data, and NIR spectra were combined into a single database. Half of the data from extensively discolored and asymptomatic kernels was randomly assigned to a training set and the other half was assigned to a validation set. All data from kernels with minor discoloration were assigned to the validation set. A stepwise discriminant analysis search was performed to find the best single feature and combination of two- and three-image or physical property features to perform a two-way classification of kernels as fungal-infected or undamaged. Only asymptomatic kernels and kernels with extensive discoloration were used to select features. The training set was used to select the features using stepwise discriminant analysis; the validation set was used to assess the classification accuracy of the discriminant function. Feature selections and classifications were made using all of the combined data as well as using each image modality, the NIR spectra, and physical properties separately.

Infecting Species Identification

Principle components of the average germ-up and germ-down spectra were computed, and the 20 principle components having the highest eigenvalues were fed as classifying features into a neural network (NeuralShell Classifier V2.01, Ward Systems Group, Inc., Frederick, Md.) to classify kernels by their infecting fungus. For this analysis, the spectra were mean-centered and then normalized by dividing each absorbance value by the average of the highest 5% of absorbance values in the entire spectra. Half of the data from asymptomatic and extensively discolored kernels were randomly assigned to a training set and the other half were assigned to a validation set. All of the kernels with minor discoloration were assigned to the validation set. The training set was used to compute the principle components and then train the neural network with these principle components. The eigenvectors computed for the principle components of the training set were applied to the validation set and used to validate the neural network classification results. The neural network training used the genetic training algorithm, as this method is much less likely to overfit the data (Lestander et

al., 2003). The training started with all 20 of the principle components. After the training was completed, the software reported the relative importance of each principle component to the classification. The least-important principle component was removed, and the training started over again. This procedure was repeated until no further improvement in classification error was observed in the training set.

RESULTS AND DISCUSSION

SUMMARY OF CLASSIFICATIONS MADE USING NIR, IMAGE, AND PHYSICAL PROPERTY DATA

Table 2 displays the classification results using each measurement type for classifying kernels as fungal-infected or undamaged. Only results from extensively discolored kernels and asymptomatic kernels are listed; results from kernels with minor discolorations as well as the use of combinations of features are discussed in more detail later. The number of features for the highest validation set accuracy and the features selected are also listed. The measurement having the highest average accuracy (given equal weighting to undamaged and fungal-infected kernels) was the NIR spectra from either the germ side or the endosperm side of the kernel. Their average accuracy was 94%. Color reflectance image data had the lowest average accuracy (82.5%). All other measurement types had average accuracies above 91%.

Kernel thickness, weight, and length had an average classification accuracy of 91.5%, on par with most of the other measurements. These features indicate that the density of fungal-infected kernels is reduced compared with undamaged kernels. The mean mass for all fungal-infected kernels was less than that of undamaged kernels at the 95% confidence level, while kernel length and thickness were not significantly different at the 95% confidence level. Additionally, the mean x-ray intensity of fungal-infected kernels was significantly lower (darker) than that of undamaged kernels at the 95% confidence level. This also indicated lower density, as the fungal-infected kernels absorbed less x-ray energy.

Table 2. Validation set classification results of fungal-infected kernels showing extensive discoloration and undamaged kernels. Classification was performed by stepwise discriminant analysis where a maximum of three features were selected.

Measurement Group	Undamaged Kernels Classified as Undamaged (%)	Fungal-Infected Kernels Classified as Infected (%)	No. of Features Selected	Features
Physical properties	93	90	3	Thickness, weight, length
NIR transmittance images (avg. of endosperm and germ sides)	93	90	3	% 780 nm pixels < 112; % 920 nm pixels < 208; and % 1020 nm pixels < 128
Color transmittance images (avg. of endosperm and germ sides)	95	89	2	% blue pixels < 64; % red pixels < 160
Color reflectance images (avg. of germ and endosperm sides)	90	75	2	Mean and maximum pixel intensity of blue image
X-ray images	100	82	3	Mean, standard deviation, and maximum pixel intensity
NIR spectra (germ side only)	97	91	3	Absorbance at 1690, 1695, and 1700 nm
NIR spectra (endosperm side only)	98	90	3	Absorbance at 535, 1690, and 1700 nm
NIR spectra (avg. of endosperm and germ sides)	98	85	3	Absorbance at 540, 780, and 1405 nm

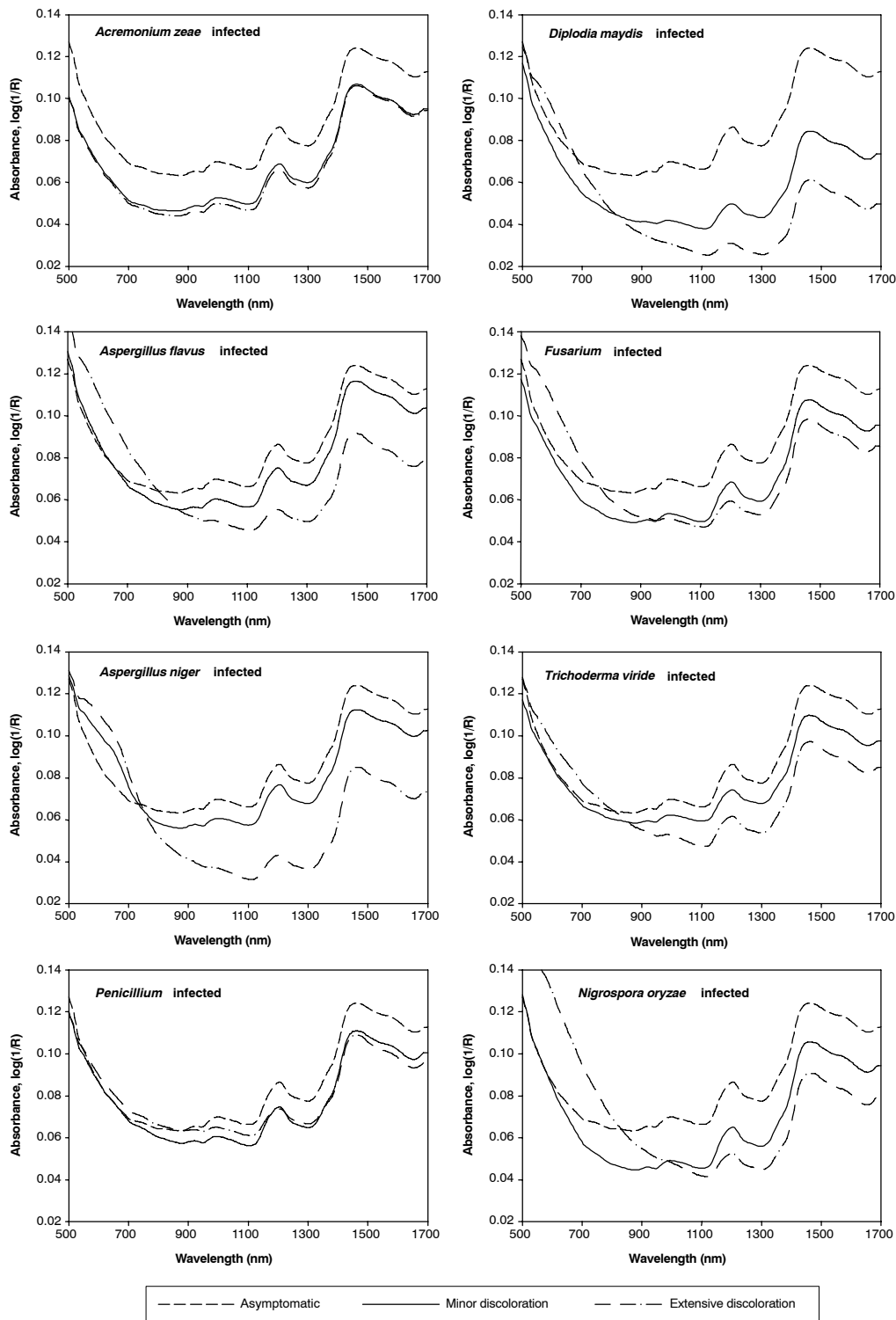


Figure 2. Plots of average spectra for fungus-infected kernels showing different symptoms of kernel discoloration (e.g., asymptomatic, minor discoloration, extensive discoloration).

Classification accuracy for fungal-infected kernels using the average of the germ and endosperm side spectra was somewhat less than the accuracy using either the germ side or endosperm side spectra alone. Features selected while using spectra from the germ side or endosperm side were absorbance values at 1690 and 1700 nm, but these were not selected from the average of the germ and endosperm spectra.

The variance of absorbance values at these wavelengths was approximately 20% higher for the average spectra than for the germ or endosperm only spectra. Both protein and starch have high absorbances at these wavelengths, and differences between the germ and endosperm in starch, and perhaps protein, content could have increased the variance of the average spectra at these wavelengths.

NIR REFLECTANCE SPECTRAL BAND SELECTION

Plots of the average reflectance spectra from kernels for each fungus and symptom category are shown in figure 2. For all fungal-infected kernels with extensive discoloration, except *A. zeae*, the absorbance of fungal-infected kernels is higher than that of undamaged kernels below 700 nm and lower between 900 and 1700 nm. (Note: in this article, we use absorbance units to represent $\log(1/R)$ data). In general, the spectra from fungal-infected kernels with minor discoloration more closely followed the spectra of asymptomatic kernels. However, the variance of individual absorbance values at each wavelength was high enough that no absorbance values from the extensively discolored and asymptomatic kernel groups were significantly different from each other at the 95% confidence level. Differences in absorbance spectra for extensively discolored kernels can possibly be explained by the scattering and absorbance characteristics caused by the fungus in the kernel. Discoloration of the kernels would cause higher visible wavelength (<~750 nm) absorbance. A fungal-infected kernel would also scatter more light than a sound, vitreous kernel, since the invasion of the fungus can cause the kernel endosperm to become porous (Hesseltine and Shotwell, 1973; Lillehoj et al., 1976). This scattering would cause less NIR radiation to be absorbed in the reflectance mode. Powdery substances with refractive indices different from that of air, such as those in the air-endosperm interface of infected kernels, cause more light to be reflected (Birth and Hecht, 1987), as opposed to the more crystalline-like property of normal kernels.

The nearest-neighbor algorithm selected the spectral bands at 715 and 965 nm as optimal for use in high-speed sorting applications. Highest accuracy was achieved when using OR logic. Use of AND logic gave considerably lower classification accuracies for fungal-damaged kernels. Validation-set classification accuracy for asymptomatic kernels was 98.1%. Average classification accuracy for all fungi types was 79.6% for extensively discolored kernels and 33.3% for kernels with minor discoloration. However, classification performance for kernels infected with *A. zeae* and *Penicillium* fungi were poor (39.3% and 17.6%, respectively). By removing these from the average computation, an average of 96.6% of the other extensively discolored kernels were correctly classified as fungal damaged, with a range between 91.7% and 100% accuracy. Table 3 lists classification results for kernels infected with all fungal types showing extensive or minor kernel discoloration. Selection of these two absorption bands indicated that fungal-damaged kernels are generally discolored, as indicated by a selection of 715 nm, and that oil concentration may be changed for fungal-damaged kernels, as indicated by the selection of the absorption band at 965 nm. These results, based on spectral band selection by the nearest-neighbor algorithm, are similar to the results from the stepwise discriminant analysis procedure where three spectral bands were selected. However, the two spectral bands and OR logic are easily implemented in commercial sorting machines, whereas averaging three spectral bands is not. Classification accuracy from stepwise selection of just two spectral bands from the average of the germ and endosperm spectra was 98% for undamaged kernels and 74% for all fungal-damaged kernels having extensive discoloration, lower than what was achieved by the nearest-neighbor algorithm.

Table 3. Percentage of visibly fungal-infected maize kernels (minor vs. extensive discoloration) in the validation set correctly classified as “fungal damaged” when using NIR absorbance values at 715 and 965 nm and OR logic from the spectral measurements from both sides of the kernel.^[a] Note that the validation set contained all of the kernels with minor discoloration and all but 30 randomly selected kernels with extensive discoloration.

Infecting Fungus	Visible Kernel Discoloration ^[b]		Kernels in Training Set
	Minor	Extensive	
<i>Acremonium zeae</i>	5.7% (89)	39.3% (19)	0
<i>Aspergillus flavus</i>	25.8% (337)	95.3% (204)	3
<i>Aspergillus niger</i>	28.8% (40)	91.7% (62)	2
<i>Diplodia maydis</i>	69.2% (181)	100% (167)	4
<i>Fusarium graminearum</i>	42.9% (73)	97.1% (63)	2
<i>Fusarium verticillioides</i>	34.7% (405)	97.2% (205)	7
<i>Penicillium</i> spp.	28.8% (45)	17.6% (88)	3
<i>Trichoderma viride</i>	30.4% (193)	98.3% (141)	9
Average of all fungi	33.3% (803)	79.6% (949)	

[a] Fungus-infected kernels selected from wound-inoculated ears of Pioneer 3394 and FS 7111 grown at Kilbourne, Illinois (see table 2). Kernels with visible symptoms of discoloration but not classified as “fungal damaged” were incorrectly classified as asymptomatic.

[b] Number of kernels examined is shown in parentheses.

A scatter plot of asymptomatic kernels and fungal-infected kernels at 715 and 965 nm is shown in figure 3. Samples infected with *A. zeae* and *Penicillium* were omitted from this plot for clarity, as samples infected with these two fungi overlap with the control kernels. Kernels infected with *A. flavus* generally have lower absorbances at 965 nm for a given absorbance at 715 nm.

Pearson et al. (2004) reported that for optimal sorting of yellow corn kernels infected with aflatoxin, a metabolite of *A. flavus*, the spectral bands centered at 750 and 1200 nm should be used. This study showed that when using these two bands (on the same spectrometer as used in the earlier study) 97% of the kernels having aflatoxin greater than 100 ppb could be separated from 100% of the kernels having no detectable aflatoxin. These spectral bands were selected on the basis of eliminating aflatoxin, not on the simple basis of fungal infections. In this study, where the objective was to detect kernels infected with fungi from a variety of species without regard to mycotoxins, 95.2% of the kernels infected with *A. flavus* and having extensive discoloration were found separable from 98% of the control kernels. Thus, classification results using the spectral pair of 715 and 965 nm for kernels infected with *A. flavus* with extensive discoloration are comparable to, but slightly less, than the classification accuracy of kernels contaminated with greater than 100 ppb aflatoxin. In Pearson et al. (2004), all but one kernel infected with greater than 100 ppb also exhibited extensive discoloration. The advantage of using the spectral pair of 715 and 965 nm is that elimination of kernels infected with several other fungi besides *A. flavus* is optimized.

CLASSIFICATIONS BASED ON COMBINED IMAGE AND PHYSICAL PROPERTY DATA

The best combination of the three features selected from all image and physical property data were all from the transmittance images. These features were the percentage of blue image pixels having an intensity below 64, percentage of red image pixels below an intensity of 160, and the percentage of pixels in the 960 nm transmittance image with an intensity below 160. These three features correctly

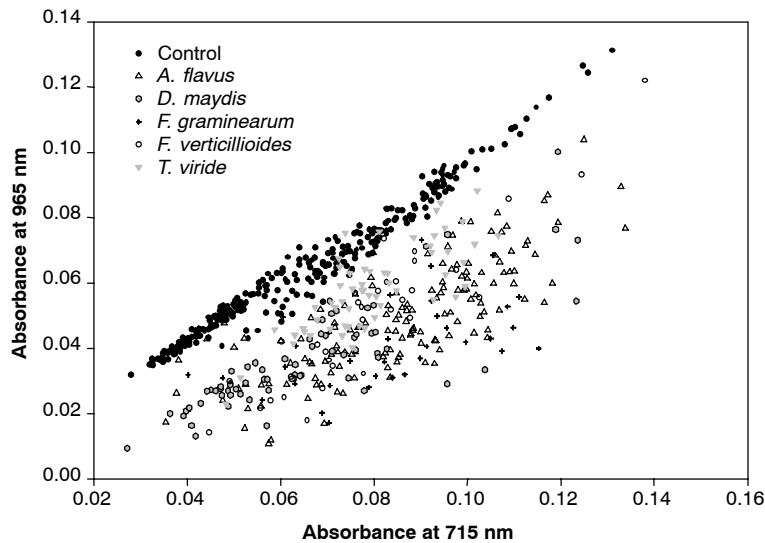


Figure 3. Scatter plot of absorbance values at 715 and 965 nm for fungus-infected kernels with extensive discoloration selected from wound-inoculated ears of Pioneer 3394 and FS 7111 grown at Kilbourne, Illinois.

classified 96.2% of the asymptomatic kernels, and among all fungal species, averaged 91.9% of those kernels showing extensive discoloration and 66.1% of kernels showing minor discoloration. This is slightly better than the classification results using two color transmittance features, but it is more difficult to measure, requiring two cameras or filter arrangements. Table 4 displays the classification accuracy for all kernels based on the infecting species using the three selected features. Note that for *Acremonium zeae* and *Penicillium* spp., the accuracy for all fungal-infected kernels, with minor or extensive discoloration, was appreciably higher using imaging than with dual-spectra bands (table 3). The accuracy of the imaging method appears to be somewhat higher for fungal-damaged kernels than the two spectral absorption values at 715 and 965 nm (table 3). However, the imaging method is not as conducive to high-speed sorting, while the reflectance from two spectral bands is more favorable. It should be noted that the two features from the color-transmittance images offered similar accuracy to the spectral method, and the hardware to acquire only color images would be

comparatively inexpensive; thus, this method may be useful for low-volume or batch inspections.

INFECTING SPECIES IDENTIFICATION BY NEURAL NETWORKS

Tables 5 through 7 show the results of classifying kernels based on the infecting species using a neural network with principle components of the average germ-up and germ-down reflectance spectra as input features. Training set error rates were minimized with 18 principle components selected. The first five principle components explained more than 98% of the spectral variance. Since the neural network used higher principle components, this suggests that minute variations in the spectra were useful for distinguishing kernels showing only minor discoloration from kernels showing extensive discoloration, as well as asymptomatic kernels. The number of principle components selected (18) is small compared to the size of the validation set: 490 extensively damaged kernels, and 1363 kernels with minor discoloration. Thus, overfitting with the neural network is not likely; however, more testing on a wider range of samples is needed to develop a robust neural network. Accuracies for extensively discolored kernels infected with *A. flavus*, *D. maydis*, *F. graminearum*, *F. verticillioides*, or *T. viride* averaged 92.1% for P-3394 corn (table 5) and 94.8% for FS-7111 corn (table 6). Classification accuracy for asymptomatic kernels with these two calibrations was 100%. When the Pioneer and Farm Service data sets were combined, classification accuracy declined somewhat: 99.1% for asymptomatic kernels, and averaging 83.4% for extensively discolored kernels infected with *A. flavus*, *D. maydis*, *F. graminearum*, *F. verticillioides*, and *T. viride* (table 7). Nevertheless, these results suggest that full-spectrum methods can be used to identify the major infecting species accurately within a corn hybrid and reasonably well across different corn hybrids and growing seasons.

Spectra of single kernels can be measured automatically and sorted into different categories using commercial instruments (e.g., Perten Instruments, Brimrose Corporation). Methods for distinguishing fungal species may be implemented by these instruments. This may be of use to breeders who need to rapidly screen samples for fungal

Table 4. Percentage of visibly fungal-infected maize kernels (minor vs. extensive discoloration) from the validation set correctly classified as “fungal damaged” when using three transmittance image features.^[a] Note that the validation set contained all of the kernels with minor discoloration and half of the kernels with extensive discoloration.

Infecting Fungus	Visible Kernel Discoloration ^[b]	
	Minor	Extensive
<i>Acremonium zeae</i>	50% (89)	88.5% (9)
<i>Aspergillus flavus</i>	53.7% (337)	97.3% (103)
<i>Aspergillus niger</i>	50% (40)	91.7% (32)
<i>Diplodia maydis</i>	98.2% (181)	100% (85)
<i>Fusarium graminearum</i>	94% (73)	97% (33)
<i>Fusarium verticillioides</i>	61% (405)	91.2% (106)
<i>Penicillium</i> spp.	65.8% (45)	78 % (46)
<i>Trichoderma viride</i>	55.7 % (193)	92.3 % (75)
Average of all fungi	66.1 % (803)	91.9 % (489)

^[a] Fungal-infected kernels selected from wound-inoculated ears of Pioneer 3394 and FS 7111 grown at Kilbourne, Illinois (see table 1). Kernels with visible symptoms of discoloration but not classified as “fungal damaged” were incorrectly classified as asymptomatic.

^[b] Number of kernels examined is shown in parentheses.

damage from different species. However, accuracies for infected kernels with minor discoloration fell by more than half compared with extensively discolored kernels. Thus, the ker-

nels need to show symptoms of extensive kernel infection in order for the infecting species to be identified by this method.

Table 5. Validation set accuracy of neural network classification for Pioneer 3394 maize kernels infected with different species of kernel-rotting fungi and showing extensive (>50%) versus minor (<50%) endosperm discoloration. Note that the validation set contained all of the kernels with minor discoloration and half of the kernels with extensive discoloration.

	No. of Kernels	Classified as						
		Asymptomatic	<i>A. flavus</i>	<i>D. maydis</i>	<i>F. graminearum</i>	<i>F. verticillioides</i>	<i>T. viride</i>	Other fungi
Extensive endosperm discoloration (>50%)								
Actual								
Asymptomatic	146	100.0%	0.0%	0.0%	0.0%	0.0%	0.0%	0.0%
<i>A. flavus</i>	74	1.4%	97.3%	0.7%	0.0%	0.7%	0.0%	0.0%
<i>D. maydis</i>	35	0.0%	2.8%	97.2%	0.0%	0.0%	0.0%	0.0%
<i>F. graminearum</i>	17	0.0%	2.9%	0.0%	94.1%	0.0%	2.9%	0.0%
<i>F. verticillioides</i>	18	0.0%	2.8%	0.0%	0.0%	83.3%	0.0%	13.9%
<i>T. viride</i>	35	0.0%	0.0%	0.0%	11.4%	0.0%	88.6%	0.0%
Other fungi								
<i>A. zeae</i>	7	0.0%	0.0%	0.0%	0.0%	7.1%	0.0%	92.9%
<i>A. niger</i>	6	0.0%	0.0%	0.0%	0.0%	0.0%	0.0%	100.0%
<i>Penicillium</i> spp. ^[a]	17	0.0%	0.0%	0.0%	2.9%	0.0%	0.0%	97.1%
Minor endosperm discoloration (<50%)								
Actual								
Asymptomatic	146	100.0%	0.0%	0.0%	0.0%	0.0%	0.0%	0.0%
<i>A. flavus</i>	299	56.5%	41.1%	0.0%	0.3%	0.7%	0.3%	1.0%
<i>D. maydis</i>	112	0.0%	14.3%	72.3%	0.9%	0.9%	6.3%	5.4%
<i>F. graminearum</i>	35	8.6%	0.0%	0.0%	51.4%	0.0%	34.3%	5.7%
<i>F. verticillioides</i>	131	14.5%	12.2%	3.1%	0.0%	30.5%	2.3%	37.4%
<i>T. viride</i>	107	29.9%	12.1%	0.9%	2.8%	2.8%	34.6%	16.8%
Other fungi								
<i>A. zeae</i>	53	9.4%	5.7%	0.0%	3.8%	1.9%	1.9%	77.4%
<i>A. niger</i>	40	0.0%	0.0%	0.0%	0.0%	2.5%	0.0%	97.5%
<i>Penicillium</i> spp. ^[a]	26	1.3%	0.0%	2.5%	17.5%	1.3%	10.0%	67.5%

[a] *P. funiculosum*, *P. oxalicum*.

Table 6. Validation set accuracy of neural network classification for FS 7111 maize kernels infected with different species of kernel-rotting fungi and showing extensive (>50%) versus minor (<50%) endosperm discoloration. Note that the validation set contained all of the kernels with minor discoloration and half of the kernels with extensive discoloration.

	No. of Kernels	Classified as						
		Asymptomatic	<i>A. flavus</i>	<i>D. maydis</i>	<i>F. graminearum</i>	<i>F. verticillioides</i>	<i>T. viride</i>	Other fungi
Extensive endosperm discoloration (>50%)								
Actual								
Asymptomatic	74	100.0%	0.0%	0.0%	0.0%	0.0%	0.0%	0.0%
<i>A. flavus</i>	29	0.0%	98.3%	0.0%	0.0%	1.7%	0.0%	0.0%
<i>D. maydis</i>	50	0.0%	0.0%	100.0%	0.0%	0.0%	0.0%	0.0%
<i>F. graminearum</i>	16	0.0%	0.0%	0.0%	90.3%	9.7%	0.0%	0.0%
<i>F. verticillioides</i>	88	2.3%	0.6%	0.6%	1.1%	88.1%	0.6%	6.8%
<i>T. viride</i>	40	0.0%	0.0%	0.0%	0.0%	2.5%	97.5%	0.0%
Other fungi								
<i>A. zeae</i>	2	0.0%	0.0%	0.0%	0.0%	0.0%	0.0%	100.0%
<i>A. niger</i>	26	0.0%	0.0%	0.0%	0.0%	0.0%	0.0%	100.0%
<i>Penicillium</i> spp. ^[a]	29	3.5%	0.0%	0.0%	0.0%	22.8%	0.0%	73.7%
Minor endosperm discoloration (<50%)								
Actual								
Asymptomatic	74	100.0%	0.0%	0.0%	0.0%	0.0%	0.0%	0.0%
<i>A. flavus</i>	38	34.2%	44.7%	2.6%	0.0%	15.8%	2.6%	0.0%
<i>D. maydis</i>	69	20.3%	0.0%	59.4%	1.4%	15.9%	2.9%	0.0%
<i>F. graminearum</i>	38	13.2%	0.0%	26.3%	5.3%	50.0%	2.6%	2.6%
<i>F. verticillioides</i>	274	31.4%	1.5%	6.2%	1.1%	43.8%	2.6%	13.5%
<i>T. viride</i>	86	5.8%	0.0%	11.6%	10.5%	27.9%	36.0%	8.1%
Other fungi								
<i>A. zeae</i>	36	61.1%	2.8%	2.8%	0.0%	22.2%	2.8%	8.3%
<i>Penicillium</i> spp. ^[a]	20	25.0%	0.0%	0.0%	0.0%	0.0%	0.0%	75.0%

[a] *P. funiculosum*, *P. oxalicum*.

Table 7. Validation set accuracy of neural network classification for Pioneer 3394 and FS 7111 (combined) maize kernels infected with different species of kernel-rotting fungi and showing extensive (>50%) versus minor (<50%) endosperm discoloration. Note that the validation set contained all of the kernels with minor discoloration and half of the kernels with extensive discoloration.

	No. of Kernels	Classified as						
		Asymptomatic	<i>A. flavus</i>	<i>D. maydis</i>	<i>F. graminearum</i>	<i>F. verticillioides</i>	<i>T. viride</i>	Other fungi
Extensive endosperm discoloration (>50%)								
Actual								
Asymptomatic	220	100.0%	0.0%	0.0%	0.0%	0.0%	0.0%	0.0%
<i>A. flavus</i>	103	2.4%	87.9%	2.9%	1.0%	2.4%	1.9%	1.4%
<i>D. maydis</i>	86	1.2%	0.0%	96.5%	0.0%	0.0%	2.3%	0.0%
<i>F. graminearum</i>	32	6.2%	4.6%	6.2%	70.8%	4.6%	3.1%	4.6%
<i>F. verticillioides</i>	106	7.5%	4.2%	4.2%	0.5%	73.1%	0.5%	9.9%
<i>T. viride</i>	75	3.3%	2.0%	2.7%	1.3%	1.3%	88.7%	0.7%
Other fungi								
<i>A. zeae</i>	9	15.8%	0.0%	0.0%	10.5%	36.8%	0.0%	36.8%
<i>A. niger</i>	32	12.5%	3.1%	1.6%	0.0%	7.8%	0.0%	75.0%
<i>Penicillium</i> spp. ^[a]	46	6.6%	3.3%	2.2%	0.0%	6.6%	0.0%	81.3%
No fungus	1	0.0%	0.0%	0.0%	0.0%	0.0%	0.0%	100%
Minor endosperm discoloration (<50%)								
Actual								
Asymptomatic	220	99.1%	0.0%	0.2%	0.0%	0.0%	0.0%	0.5%
<i>A. flavus</i>	337	67.4%	13.9%	0.9%	0.9%	4.5%	7.1%	5.3%
<i>D. maydis</i>	181	29.8%	0.6%	34.3%	1.1%	6.1%	21.5%	6.6%
<i>F. graminearum</i>	73	49.3%	1.4%	8.2%	17.8%	5.5%	8.2%	9.6%
<i>F. verticillioides</i>	405	52.1%	1.7%	4.0%	0.7%	15.3%	3.2%	23.0%
<i>T. viride</i>	193	5.8%	0.0%	11.6%	10.5%	27.9%	36.0%	8.1%
Other fungi								
<i>A. zeae</i>	89	71.9%	2.2%	0.0%	3.4%	4.5%	6.7%	11.2%
<i>A. niger</i>	40	0.0%	37.5%	2.5%	0.0%	5.0%	0.0%	55.0%
<i>Penicillium</i> spp. ^[a]	100	30.0%	2.0%	0.0%	9.0%	8.0%	12.0%	39.0%
No fungus	38	60.5	0.0%	5.3%	0.0%	7.9%	2.6%	23.7%

[a] *P. funiculosum*, *P. oxalicum*.

CONCLUSION

It was found that multi-spectral transmittance imaging, physical properties, and reflectance spectroscopy are all viable tools for discriminating corn kernels infected with various fungi from un-infected controls; each modality had classification accuracies above 91%. Kernels infected with one of several fungi can be distinguished from un-infected controls using reflectance values at just two wavelengths using the same decision logic as is used in high-speed optical sorters. Two- or three-image histogram features from visible and near-infrared transmittance images can also correctly identify severely damaged kernels due to fungal infection with good accuracy; however, implementation is more difficult than the use of two spectral bands in commercial high-speed sorters. Full-spectrum methods are needed to identify infecting fungal species. These results indicate that this technology can potentially be used to automatically and rapidly detect fungal-infected corn kernels. This may be of great assistance to breeders who are interested in developing fungal-resistant varieties.

ACKNOWLEDGEMENTS

The authors wish to thank Carrie Schwartz for excellent technical assistance. Mention of trade names or commercial products in this publication is solely for the purpose of providing specific information and does not imply recommendation or endorsement by the USDA.

REFERENCES

- Bennett, G. A., D. T. Wicklow, R. W. Caldwell, and E. B. Smalley. 1988. Distribution of trichothecenes and zearalenone in *Fusarium graminearum*: Rotted corn ears grown in a controlled environment. *J. Agric. Food Chem.* 36(3): 639-642.
- Birth, G. S., and H. G. Hecht. 1987. The physics of near-infrared reflectance. In *Near-Infrared Technology in the Agriculture and Food Industries*, 1-15. P. Williams and K. Norris, eds. St. Paul, Minn.: American Association of Cereal Chemists.
- Brekke, O. L., A. F. Peplinski, G. E. N. Nelson, and E. L. Griffin. 1975. Cleaning trials for corn containing aflatoxin. *Cereal Chem.* 52(2): 198-204.
- Caldwell, R. W., J. F. Tuite, and W. W. Carlton. 1981. Pathogenicity of penicillia to corn ears. *Phytopathology* 71(1): 175-180.
- Christensen, C. M., and H. H. Kaufmann. 1969. *Grain Storage: The Role of Fungi in Quality Loss*. Minneapolis, Minn.: University of Minnesota Press.
- Clayton, E. E. 1927. *Diplodia* ear-rot disease of corn. *J. Agric. Res.* 34: 357-371.
- Clements, M. J., K. W. Campbell, C. M. Maragos, C. Pilcher, J. M. Headrick, J. K. Pataky, and D. G. White. 2003. Influence of Cry1Ab protein and hybrid genotype on fumonisin contamination and *Fusarium* ear rot of corn. *Crop Sci.* 43(4): 1283-1293.
- Dowell, F. E., T. C. Pearson, E. B. Maghirang, F. Xie, and D. T. Wicklow. 2002. Reflectance and transmittance spectroscopy applied to detecting fumonisin in single corn kernels infected with *Fusarium verticillioides*. *Cereal Chem.* 79(2): 222-226.
- Faraq, R. S., A. M. Youssef, K. A. Sabet, M. M. Fahim, and F. A. Khalil. 1981. Chemical studies on corn embryos infected by various fungi, *Aspergillus*, *Fusarium moniliforme*, and *Penicillium oxalicum*. *J. American Oil Chem. Soc.* 58(6): 722-728.

- Hart, L. P., E. Gendloff, and E. C. Rossman. 1984. Effect of corn genotypes on ear rot infection by *Gibberella zeae*. *Plant Dis.* 68(4): 296-298.
- Hesseltine, C. W., and O. L. Shotwell. 1973. New methods for rapid detection of aflatoxin. *Pure and Appl. Chem.* 35(3): 259-266.
- Johann, H. 1935. Histology of the caryopsis of yellow dent corn, with reference to resistance and susceptibility to kernel rot. *J. Agric. Res.* 51: 855-883.
- Klapproth, J. C., and J. A. Hawk. 1991. Evaluation of four inoculation techniques for infecting corn ears with *Stenocarpella maydis*. *Plant Dis.* 75(10): 1057-1060.
- Koehler, B. 1942. Natural mode of entrance of fungi into corn ears and some symptoms that indicate infection. *J. Agric. Res.* 64: 421-422.
- Lambert, R. J., and D. G. White. 1997. Disease reaction changes from tandem selection for multiple disease resistance in two maize synthetics. *Crop Science* 37(1): 66-69.
- Lawrence, E. B., P. E. Nelson, and J. E. Ayers. 1981. Histopathology of sweet corn seed and plants infected with *Fusarium moniliforme* and *F. oxysporum*. *Phytopathology* 71(4): 379-386.
- Lestander, T. A., R. Leardi, and P. Geladi. 2003. Selection of near-infrared wavelengths using genetic algorithms for the determination of seed moisture content. *J. Near-Infrared Spectrosc.* 11(4): 433-446.
- Lillehoj, E. B., W. F. Kwolek, R. E. Peterson, O. L. Shotwell, and C. W. Hesseltine. 1976. Aflatoxin contamination, fluorescence, and insect damage in corn infected with *Aspergillus flavus* before harvest. *Cereal Chem.* 53(4): 505-512.
- Munkvold, G. P., D. C. McGee, and W. M. Carlton. 1997. Importance of different pathways for maize kernel infection by *Fusarium moniliforme*. *Phytopathology* 87(2): 209-217.
- Naidoo, G., A. M. Forbes, C. Paul, D. G. White, and T. R. Rocheford. 2002. Resistance to *Aspergillus* ear rot and aflatoxin accumulation in maize F1 hybrids. *Crop Sci.* 42(2): 360-364.
- Pearson, T. C., D. T. Wicklow, E. B. Maghirang, F. Xie, and F. E. Dowell. 2001. Detecting aflatoxin in single corn kernels by near-infrared transmittance and reflectance spectroscopy. *Trans. ASAE* 44(5): 1247-1254.
- Pearson, T. C., D. T. Wicklow, and M. C. Pasikatan. 2004. Reduction of aflatoxin and fumonisin contamination in yellow corn by high-speed dual-wavelength sorting. *Cereal Chem.* 81(4): 490-498.
- Pomeranz, Y. 1992. Biochemical, functional, and nutritive changes during storage. In *Storage of Cereal Grains and Their Products*, 55-141. 4th ed. D. B. Sauer, ed. St. Paul, Minn.: American Association of Cereal Chemists.
- Richard, J. L., and G. A. Payne. 2003. Mycotoxins: Risks in plant, animal, and human systems. CAST Task Force Report No. 139. Ames, Iowa: Council for Agricultural Science and Technology.
- Richard-Molard, D. 1988. General characteristics of the microflora of grains and seeds and the principal resulting spoilages. In *Preservation and Storage of Grains, Seeds and Their Byproducts*, 226-243. J. L. Multon, ed. New York, N.Y.: Lavoisier Publishing.
- Samuels, G. J. 1984. Toxicogenic fungi as Ascomycetes. In *Toxigenic Fungi: Their Toxins and Health Hazard*, 119-128. H. Kurata and Y. Ueno, eds. Amsterdam, The Netherlands: Elsevier Science.
- Sauer, D. B., and C. M. Christensen. 1969. Some factors affecting increase in fat acidity values in corn. *Phytopathology* 59(1): 108-110.
- Shetty, P. H., and R. V. Bhat. 1999. A physical method for segregation of fumonisin-contaminated maize. *Food Chem.* 66(3): 371-374.
- Shotwell, O. L., M. L. Goulden, and C. W. Hesseltine. 1974. Aflatoxin: Distribution in contaminated corn. *Cereal Chem.* 51(4): 492-499.
- Smart, M. J., D. T. Wicklow, and R. W. Caldwell. 1990. Pathogenesis in *Aspergillus* ear rot of maize: Light microscopy of fungal spread from wounds. *Phytopathology* 80(12): 1287-1294.
- Smith, I. M., J. Dunez, R. A. Lelliott, D. H. Phillips, and S. A. Archer, eds. 1988. *European Handbook of Plant Diseases*. Oxford, U.K.: Blackwell Science.
- Sutton, J. C. 1982. Epidemiology of wheat head blight and maize ear rot caused by *Fusarium graminearum*. *Canadian J. Plant Pathol.* 4(2): 195-209.
- Wacowicz, E. 1991. Changes of chemical grain components, especially lipids, during their deterioration by fungi. In *Cereal Grain: Mycotoxins, Fungi, and Quality in Drying and Storage*, 259-280. J. Chelkowski, ed. Amsterdam, The Netherlands: Elsevier.
- Walker, R. D., and D. G. White. 2001. Inheritance of resistance to *Aspergillus* ear rot and aflatoxin production of corn for C12. *Plant Dis.* 85(3): 322-327.
- White, D. G. 1999. *Compendium of Corn Diseases*. 3rd ed. St. Paul, Minn.: American Phytopathological Society Press.
- Wicklow, D. T. 1995. The mycology of stored grain: An ecological perspective. In *Stored Grain Ecosystems*, 197-249. D. S. Jayas, N. D. G. White, and W. E. Muir, eds. New York, N.Y.: Marcel Dekker.
- Wicklow, D. T., C. W. Hesseltine, O. L. Shotwell, and G. L. Adams. 1980. Interference competition and aflatoxin levels in corn. *Phytopathology* 70(8): 761-764.
- Wright, W. R., and B. A. Billeter. 1974. Red kernel disease of sweet corn on the retail market. *Plant Dis. Rep.* 58(12): 1065-1066.

